

# Variable Coordination Modes of Benzaldehyde Thiosemicarbazones – Synthesis, Structure, and Electrochemical Properties of Some Ruthenium Complexes

Swati Dutta,<sup>[a]</sup> Falguni Basuli,<sup>[a]</sup> Alfonso Castineiras,<sup>[b]</sup> Shie-Ming Peng,<sup>[c]</sup>  
Gene-Hsiang Lee,<sup>[c]</sup> and Samareh Bhattacharya\*<sup>[a]</sup>

**Keywords:** Thiosemicarbazones / S ligands / N ligands / Ruthenium / Coordination modes

Reaction of benzaldehyde thiosemicarbazones [ $H_2LR$ , where  $H_2$  stands for the two protons, the hydrazinic proton, and the phenyl proton at the *ortho* position, with respect to the imine function and  $R$  ( $R = OCH_3, CH_3, H, Cl$ , and  $NO_2$ ) for the *para* substituent] with  $[Ru(PPh_3)_2(CO)_2Cl_2]$ , carried out in refluxing ethanol, afforded monomeric complexes of type  $[Ru(PPh_3)_2(CO)(HLR)(H)]$ . The crystal structure of the  $[Ru(PPh_3)_2(CO)(HLNO_2)(H)]$  complex was determined. The thiosemicarbazone ligand is coordinated to the ruthenium center as a bidentate N,S-donor ligand forming a four-membered chelate ring. When the reaction of the thiosemicarbazones with  $[Ru(PPh_3)_2(CO)_2Cl_2]$  was carried out in refluxing toluene, a family of dimeric complexes of type  $[Ru_2(PPh_3)_2(CO)_2(LR)_2]$  were obtained. The crystal structure of  $[Ru_2(PPh_3)_2(CO)_2(LCl)_2]$  was determined. Each thiosemicarbazone ligand is coordinated to one ruthenium atom, by disso-

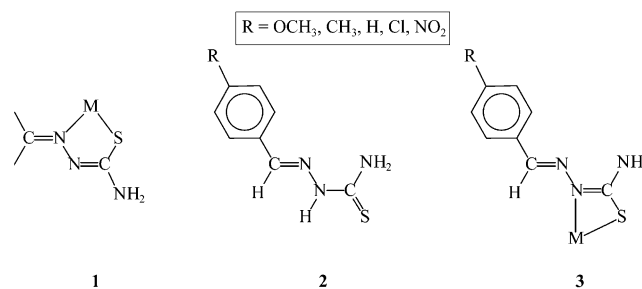
ciation of the two protons, as a dianionic tridentate C,N,S-donor ligand, and at the same time the sulfur atom is also bonded to the second ruthenium center.  $^1H$  NMR spectra of the complexes of both types are in excellent agreement with their compositions. All the dimeric and monomeric complexes are diamagnetic (low-spin  $d^6$ ,  $S = 0$ ) and show intense absorptions in the visible and ultraviolet regions. Cyclic voltammetry of the  $[Ru(PPh_3)_2(CO)(HLR)(H)]$  and  $[Ru_2(PPh_3)_2(CO)_2(LR)_2]$  complexes show the ruthenium(II)–ruthenium(III) oxidation within 0.48–0.73 V vs. SCE followed by a ruthenium(III)–ruthenium(IV) oxidation within 1.09–1.47 V vs. SCE. Potentials of both the oxidations are found to correlate linearly with the electron-withdrawing character of the substituent  $R$ .

(© Wiley-VCH Verlag GmbH & Co. KGaA, 69451 Weinheim, Germany, 2008)

## Introduction

The chemistry of transition-metal complexes of thiosemicarbazone ligands has been receiving considerable attention primarily because of their bioinorganic relevance<sup>[1]</sup> in general and for their biological (viz. antibacterial, antimalarial, antiviral, and antitumor) activities<sup>[2]</sup> in particular. We have been exploring the chemistry of thiosemicarbazone complexes of the platinum metals<sup>[3]</sup> mainly with the objective of manipulating the different possible coordination modes of the thiosemicarbazone ligands in their complexes, and the present work has originated from this exploration. Thiosemicarbazones are usually expected to bind to a metal ion, by loss of the hydrazinic proton, as monoanionic bidentate N,S-donor ligands forming five-membered chelate rings (as

in **1**), which is indeed the case for several ligands of this family.<sup>[4]</sup> However, we have observed that in their reactions with ruthenium and osmium, benzaldehyde thiosemicarbazones **2** display a rather unusual coordination mode (**3**) where they form four-membered chelate rings.<sup>[3a–3c]</sup>



Such a mode of coordination is also known for some other thiosemicarbazones.<sup>[5]</sup> Our search for the reason behind such an unusual mode of binding (as in **3**) has revealed that five-membered chelate ring formation (as shown in **1**) is not possible for benzaldehyde thiosemicarbazones, because they have a rigid geometry across the C=N bond (as shown in **2**), and in case they are forced to form a five-membered chelate ring, the phenyl ring comes close to the metal center (as shown in **4**) and thus creates an unavoidable

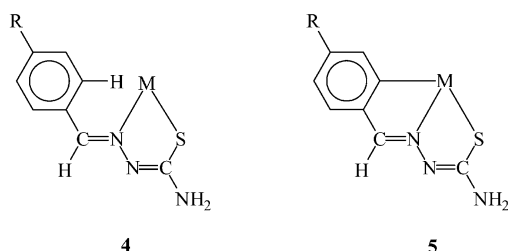
[a] Department of Chemistry, Inorganic Chemistry Section, Jadavpur University, Kolkata 700032, India  
E-mail: samareh\_b@hotmail.com

[b] Departamento de Química Inorgánica, Universidad de Santiago de Compostela, 15782 Santiago de Compostela, Spain

[c] Department of Chemistry, National Taiwan University, Taipei, Taiwan, ROC

Supporting information for this article is available on the WWW under <http://www.eurjic.org> or from the author.

able steric problem.<sup>[3c]</sup> It is relevant to mention here that we have not been able to find a single example of a structurally characterized benzaldehyde thiosemicarbazone complex in the literature, in which the ligand is coordinated as in **4**. However, closeness of the phenyl ring to the metal center in this sterically unfavorable coordination mode (as in **4**) points to the possibility of *ortho*-metalation of the phenyl ring (as in **5**) by C–H bond activation under suitable reaction conditions. The present study was initiated to explore such a possibility by using ruthenium as the metal and a group of five benzaldehyde thiosemicarbazones **2**, differing in the *para* substituent R (R = OCH<sub>3</sub>, CH<sub>3</sub>, H, Cl, and NO<sub>2</sub>) of the phenyl ring, as the ligands.



These ligands are abbreviated in general as H<sub>2</sub>LR, where H<sub>2</sub> stands for the two protons [the phenyl proton at the *ortho* position with respect to the azomethine group and the hydrazininc N–H proton, which were expected to undergo dissociation during complexation in the C,N,S-mode (**5**)] and R for the *para* substituent. These *para* substituents with a gradual variation in their inductive effect are chosen in order to study their influence, if any, on the metal-centered redox potentials. As the ruthenium starting material, the [Ru(PPh<sub>3</sub>)<sub>2</sub>(CO)<sub>2</sub>Cl<sub>2</sub>] complex was selected, particularly because in its reaction with benzaldehyde semicarbazones it was found to be very useful in affording complexes where the coordination mode of the semicarbazones could be manipulated by simple variation of the experimental conditions.<sup>[6]</sup> Reaction of [Ru(PPh<sub>3</sub>)<sub>2</sub>(CO)<sub>2</sub>Cl<sub>2</sub>] with benzaldehyde thiosemicarbazones **2** indeed has afforded complexes of two different types, and herein we report the chemistry of these two groups of complexes, with special reference to their formation, structure, and electrochemical properties.

## Results and Discussion

Reaction of the benzaldehyde thiosemicarbazones (H<sub>2</sub>LR, **2**) with [Ru(PPh<sub>3</sub>)<sub>2</sub>(CO)<sub>2</sub>Cl<sub>2</sub>], carried out in refluxing ethanol, afforded a group of complexes of the type [Ru(PPh<sub>3</sub>)<sub>2</sub>(CO)(HLR)(H)] in good yields. Elemental (C, H, N) analytical data of the complexes agree well with their compositions. It is interesting to note here that a hydride ion is coordinated to ruthenium in all these complexes and the solvent (ethanol) appears to have served as the source of this hydride. Conversion of a Ru–Cl bond into a Ru–H bond in alcoholic medium has precedent in the literature.<sup>[7]</sup> Indirect support of this speculation comes from the fact that similar reactions carried out in toluene do not afford any hydride complex (*vide infra*). To elucidate the coordina-

tion mode of the benzaldehyde thiosemicarbazones in these [Ru(PPh<sub>3</sub>)<sub>2</sub>(CO)(HLR)(H)] complexes, the structure of a representative complex, viz. [Ru(PPh<sub>3</sub>)<sub>2</sub>(CO)(HLNO<sub>2</sub>)(H)], was determined by X-ray crystallography. The structure is shown in Figure 1 and selected bond parameters are presented in Table 1. The thiosemicarbazone ligand is coordi-

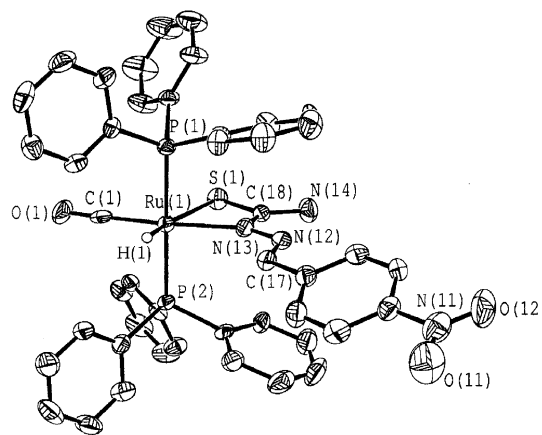


Figure 1. View of the [Ru(PPh<sub>3</sub>)<sub>2</sub>(CO)(HLNO<sub>2</sub>)(H)] complex.

Table 1. Selected bond lengths and angles for [Ru(PPh<sub>3</sub>)<sub>2</sub>(CO)(HLNO<sub>2</sub>)(H)]·CH<sub>3</sub>CN and [Ru<sub>2</sub>(PPh<sub>3</sub>)<sub>2</sub>(CO)<sub>2</sub>(LCl)<sub>2</sub>]·2CH<sub>2</sub>Cl<sub>2</sub>.

[Ru(PPh <sub>3</sub> ) <sub>2</sub> (CO)(HLNO <sub>2</sub> )(H)]·CH <sub>3</sub> CN			
Bond lengths [Å]		Bond angles [°]	
Ru(1)–C(1)	1.864(8)	P(1)–Ru(1)–P(2)	172.55(8)
Ru(1)–N(13)	2.157(6)	C(1)–Ru(1)–N(13)	172.9(3)
Ru(1)–P(1)	2.344(2)	O(1)–C(1)–Ru(1)	179.3(7)
Ru(1)–P(2)	2.351(2)	S(1)–Ru(1)–H(1)	163.0(19)
Ru(1)–S(1)	2.545(2)	C(18)–N(13)–Ru(1)	103.8(5)
Ru(1)–H(1)	1.58(6)	C(18)–S(1)–Ru(1)	78.9(3)
N(12)–N(13)	1.384(7)	N(13)–Ru(1)–S(1)	64.23(17)
N(12)–C(17)	1.285(8)	N(13)–C(18)–S(1)	113.0(6)
N(13)–C(18)	1.309(8)		
C(18)–S(1)	1.703(7)		
N(14)–C(18)	1.348(8)		
[Ru <sub>2</sub> (PPh <sub>3</sub> ) <sub>2</sub> (CO) <sub>2</sub> (LCl) <sub>2</sub> ]·2CH <sub>2</sub> Cl <sub>2</sub>			
Bond lengths [Å]		Bond angles [°]	
Ru(1)–C(1)	1.857(3)	C(1)–Ru(1)–N(1)	173.29(11)
Ru(1)–C(10)	2.050(3)	P(1)–Ru(1)–S(2)	172.34(3)
Ru(1)–N(1)	2.092(2)	C(10)–Ru(1)–S(1)	157.19(8)
Ru(1)–P(1)	2.3071(7)	Ru(1)–S(1)–Ru(2)	93.24(2)
Ru(1)–S(1)	2.4786(7)	C(3)–S(1)–Ru(1)	95.84(10)
Ru(1)–S(2)	2.4804(7)	C(3)–S(1)–Ru(2)	108.59(9)
C(1)–O(1)	1.153(4)	C(2)–Ru(2)–N(4)	171.48(11)
C(3)–S(1)	1.781(3)	P(2)–Ru(2)–S(1)	168.84(3)
C(4)–N(1)	1.294(4)	C(18)–Ru(2)–S(2)	156.84(8)
N(1)–N(2)	1.389(3)	Ru(2)–S(2)–Ru(1)	93.40(2)
Ru(2)–C(2)	1.857(3)	C(11)–S(2)–Ru(2)	95.97(10)
Ru(2)–C(18)	2.056(3)	C(11)–S(2)–Ru(1)	111.16(10)
Ru(2)–N(4)	2.098(2)		
Ru(2)–P(2)	2.3082(8)		
Ru(2)–S(2)	2.4709(7)		
Ru(2)–S(1)	2.4795(7)		
C(2)–O(2)	1.148(4)		
C(11)–S(2)	1.783(3)		
C(12)–N(4)	1.284(4)		
N(4)–N(5)	1.398(3)		

nated to ruthenium as a monoanionic bidentate N,S-donor ligand forming a four-membered chelate ring (e.g., **3**) with a bite angle of 113.0(9)°. Formation of such a four-membered chelate ring by the benzaldehyde thiosemicarbazone and similar ligands is quite normal.<sup>[3,5]</sup> Ruthenium has a HCNP<sub>2</sub>S coordination sphere in this complex, which is distorted octahedral in nature as indicated by the bond parameters around the ruthenium center. The thiosemicarbazone ligand, ruthenium, carbonyl, and hydride constitute one equatorial plane of the octahedron with the metal at the center, and the two triphenylphosphane ligands take up the remaining two axial positions; hence, they are mutually *trans*. The carbonyl is *trans* to the coordinated nitrogen atom of the thiosemicarbazone and the hydride is *trans* to the sulfur atom. In complexes of ruthenium(II) containing the Ru(PPh<sub>3</sub>)<sub>2</sub> fragment, the PPh<sub>3</sub> ligands usually occupy mutually *cis* positions for optimum  $\pi$  interaction.<sup>[8]</sup> However, in the present group of complexes they are mutually *trans*, probably due to steric reasons as well as the presence of the stronger  $\pi$  acid CO. The Ru–H, Ru–C(CO), and Ru–P distances are normal, as reported in structurally characterized complexes of ruthenium(II) containing these bonds.<sup>[9]</sup> Within the Ru(HLNO<sub>2</sub>) fragment the Ru–N length is comparable to that found in similar four-membered chelates,<sup>[3a–3c]</sup> whereas the Ru–S distance is a little longer than usually observed. The elongation of the Ru–S bond, which is *trans* to the Ru–H bond, may be attributed to the *trans* effect of the hydride ligand. Comparison of the bond lengths in the coordinated thiosemicarbazone ligand with those in the uncoordinated ligand<sup>[3c]</sup> shows that upon coordination the C–S bond has undergone elongation, whereas the adjacent C–N bond has undergone contraction. These changes in bond lengths are consistent with the iminothiolate form of the thiosemicarbazone ligand that appears to be stabilized upon coordination to the metal through loss of the hydrazinic proton.

In the crystal lattice of the [Ru(PPh<sub>3</sub>)<sub>2</sub>(CO)(HLNO<sub>2</sub>)(H)] complex there is one molecule of acetonitrile per complex molecule. In order to discover any noncovalent interactions in the lattice in general, and the link between the solvent molecule and the complex molecules in particular, the packing pattern in the lattice was scrutinized, and it shows that hydrogen-bonding interactions of three types, viz. C–H $\cdots$ O, C–H $\cdots$ S, and N–H $\cdots$ N, are active in the lattice (Figure 2, Table S1). One oxygen atom of the nitro group of each molecule is hydrogen bonded to a phenyl hydrogen of a PPh<sub>3</sub> belonging to a neighboring complex molecule leading to a strong intermolecular interaction (Figure 2a). One methyl hydrogen of the acetonitrile is hydrogen bonded to the sulfur atom of a coordinated thiosemicarbazone of a complex molecule, whereas the nitrogen atom of the same acetonitrile is hydrogen bonded to a hydrogen atom of the NH<sub>2</sub> group of a second complex molecule (Figure 2b). Thus, the acetonitrile bridges two complex molecules through strong intermolecular interactions. These extended hydrogen-bonding interactions seem to be responsible for holding the crystal together. It may be relevant to note here that such hydrogen-bonding interactions are of significant

importance in molecular recognition processes as well as in crystal engineering.<sup>[10]</sup> As all the [Ru(PPh<sub>3</sub>)<sub>2</sub>(CO)(HLR)(H)] complexes were synthesized similarly, and as they display similar properties (vide infra), the other four [Ru(PPh<sub>3</sub>)<sub>2</sub>(CO)(HLR)(H)] (R  $\neq$  NO<sub>2</sub>) complexes are assumed to have a structure similar to that of [Ru(PPh<sub>3</sub>)<sub>2</sub>(CO)(HLNO<sub>2</sub>)(H)].

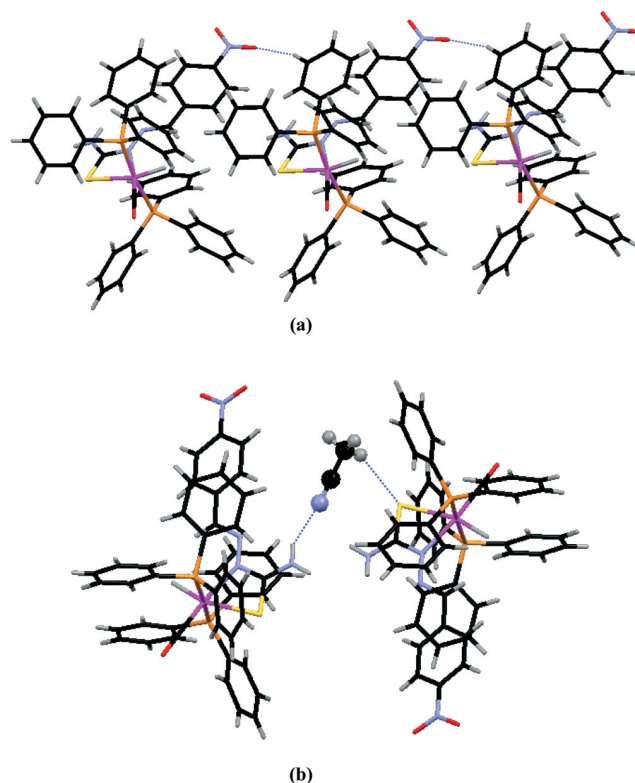


Figure 2. The hydrogen bonding interactions in the crystal lattice of [Ru(PPh<sub>3</sub>)<sub>2</sub>(CO)(HLNO<sub>2</sub>)(H)]: (a) C–H $\cdots$ O and (b) C–H $\cdots$ N and C–H $\cdots$ S interactions.

Facile formation of the hydride complexes in ethanol prompted us to try other solvents that cannot serve as hydride sources. The fact that the benzaldehyde semicarbazone ligands displayed different coordination modes in their reaction with [Ru(PPh<sub>3</sub>)<sub>2</sub>(CO)<sub>2</sub>Cl<sub>2</sub>] under different reaction conditions has further boosted this idea.<sup>[6]</sup> Encouraged by these ideas, reaction of benzaldehyde thiosemicarbazone ligands **2** with [Ru(PPh<sub>3</sub>)<sub>2</sub>(CO)<sub>2</sub>Cl<sub>2</sub>] has also been carried out in refluxing toluene, wherefrom a new series of orange complexes were obtained in decent yields. Elemental (C, H, N) analytical data of the complexes could not help us to know the composition of the complexes. To know the composition structural characterization was done of a representative member of this family by X-ray crystallography. The structure is shown in Figure 3 and selected bond parameters are given in Table 1. The structure reveals that the complex is dimeric, where each monomeric unit consists of a square-pyramidal Ru(PPh<sub>3</sub>)<sub>3</sub>(CO)(LCl) moiety. The Ru(CO)(LCl) fragment constitutes the square base with the metal at the center and the PPh<sub>3</sub> ligand takes up the apical position. The thiosemicarbazone ligand is coordinated to ruthenium as a

dianionic tridentate C,N,S-donor ligand by dissociation of two protons forming two five-membered chelate rings. Two such monomeric units are bridged by the sulfur atoms of the thiosemicarbazone ligands (as in **6**). Hence, the benzaldehyde thiosemicarbazone ligands are actually serving as tetradentate ligands in these complexes.

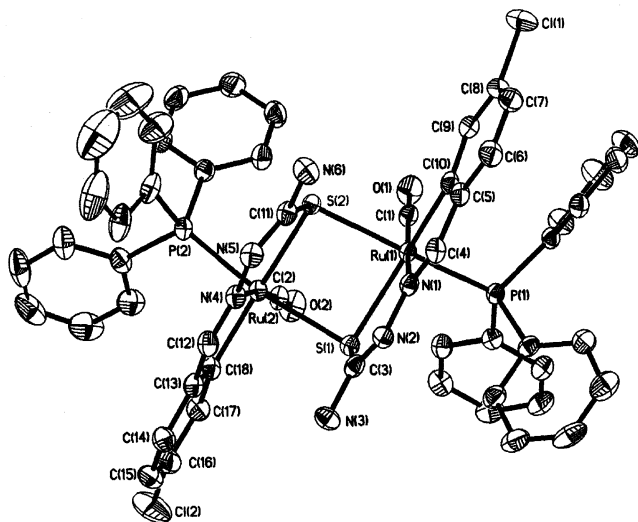
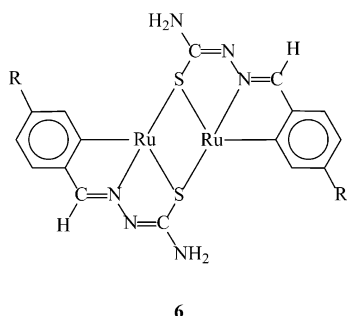


Figure 3. View of the  $[\text{Ru}_2(\text{PPh}_3)_2(\text{CO})_2(\text{LCl})_2]$  complex.



There are only a few examples known where such a coordination mode is displayed by the benzaldehyde thiosemicarbazone ligands.<sup>[11]</sup> Each ruthenium is sitting at the center of a  $\text{C}_2\text{NPS}_2$  coordination sphere, which is distorted from ideal octahedral geometry, as reflected in the bond parameters around each ruthenium atom. Although the  $\text{Ru}-\text{C}(\text{CO})$  distance is similar to that observed in the previous structure, the  $\text{Ru}-\text{P}$  length is a bit shorter,<sup>[12]</sup> which is attributable to a stronger  $\pi$  interaction in the  $\text{Ru}(\text{PPh}_3)$  fragments of this complex. This interaction was weaker in the previous complex for the *trans* disposition of the two  $\text{PPh}_3$  ligands. The observed  $\text{Ru}-\text{C}$ ,  $\text{Ru}-\text{N}$ , and  $\text{Ru}-\text{S}$  distances are quite normal.<sup>[1,3a,6]</sup> Comparison of bond lengths with those of the uncoordinated thiosemicarbazone ligand<sup>[3c]</sup> shows that significant changes have taken place in the  $\text{S}-\text{C}-\text{N}-\text{N}-\text{C}-\text{Ru}$  fragment of the ligand upon its coordination to the metal by dissociation of the two protons. In the crystal lattice there are two molecules of dichloromethane per molecule of the dimeric complex. The packing pattern in the lattice (Figure 4, Table S1) shows that one of the two dichloromethane molecules is bridging two dimeric mole-

cules through  $\text{C}-\text{H}\cdots\text{S}$ ,  $\text{C}-\text{H}\cdots\text{Cl}$ , and  $\text{C}-\text{Cl}\cdots\pi$  interactions. The same dichloromethane molecule is also linked to the second dichloromethane molecule through a  $\text{C}-\text{H}\cdots\text{Cl}$  interaction (Figure 4a). Additionally, there also exists intermolecular  $\text{C}-\text{H}\cdots\text{O}$  and  $\text{C}-\text{H}\cdots\pi$  interactions (Figure 4b). In view of the similarity in synthetic procedures and properties (vide infra), the other four  $[\text{Ru}_2(\text{PPh}_3)_2(\text{CO})_2(\text{LR})_2]$  ( $\text{R} \neq \text{Cl}$ ) complexes are assumed to have a structure similar to that of  $[\text{Ru}_2(\text{PPh}_3)_2(\text{CO})_2(\text{LCl})_2]$ .

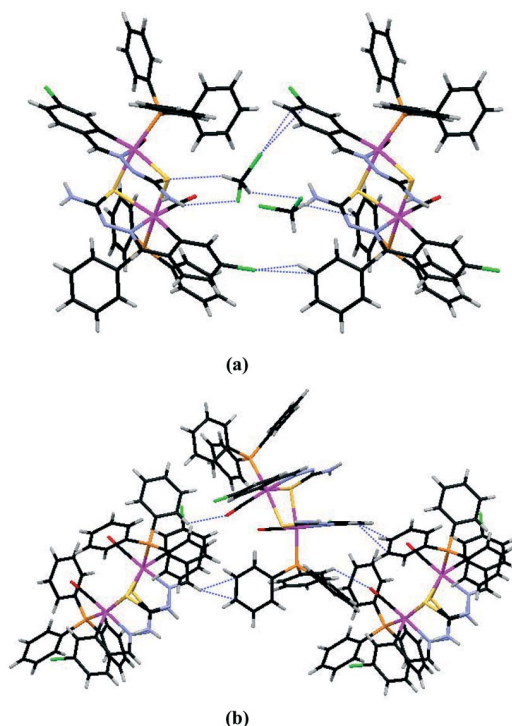
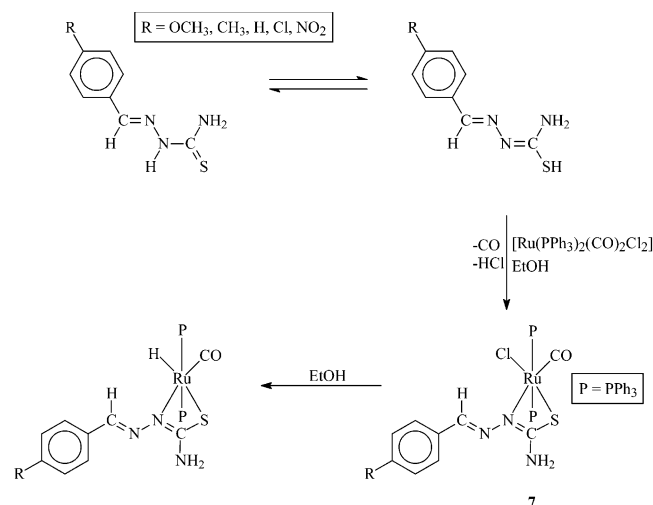


Figure 4. Hydrogen-bonding interactions in the crystal lattice of  $[\text{Ru}_2(\text{PPh}_3)_2(\text{CO})_2(\text{LCl})_2]$ : (a)  $\text{C}-\text{H}\cdots\text{S}$ ,  $\text{C}-\text{H}\cdots\text{Cl}$  and  $\text{C}-\text{Cl}\cdots\pi$ , and (b)  $\text{C}-\text{H}\cdots\text{O}$  and  $\text{C}-\text{H}\cdots\pi$  interactions.

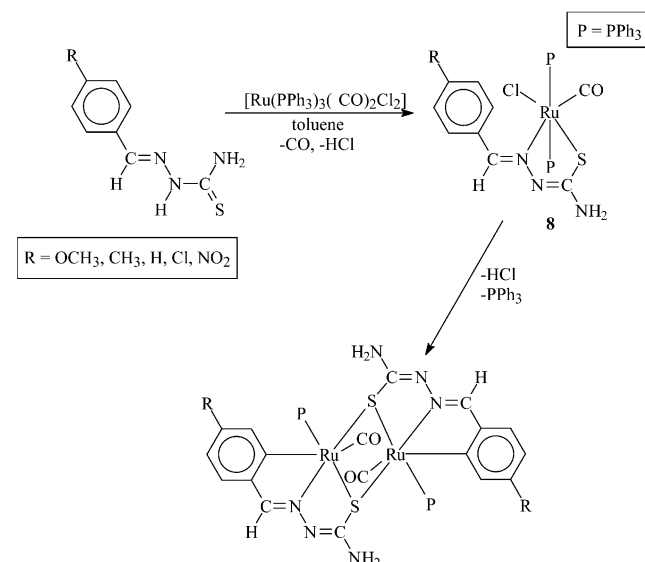
The mechanisms for the formation of the two types of complexes are not completely clear to us, but the sequences shown in Schemes 1 and 2 seem probable. In solution the benzaldehyde thiosemicarbazones are known to exist in two tautomeric thione and thiol forms. In ethanol, the thiol tautomer is likely to be the dominant species, which reacts with  $[\text{Ru}(\text{PPh}_3)_2(\text{CO})_2\text{Cl}_2]$  to afford complex **7** by elimination of  $\text{CO}$  and  $\text{HCl}$ . In **7**, the thiosemicarbazone ligand is coordinated as an N,S-donor ligand forming a four-membered chelate ring. Subsequently, the  $\text{Ru}-\text{Cl}$  bond is converted into a  $\text{Ru}-\text{H}$  bond under prevailing reaction conditions to give the final product.<sup>[7]</sup> However, in toluene the thione tautomer appears to be more dominant and it reacts with  $[\text{Ru}(\text{PPh}_3)_2(\text{CO})_2\text{Cl}_2]$  to form reactive intermediate **8**, in which the ligand is bound to ruthenium as an N,S-donor ligand forming a five-membered ring. Intermediates **7** and **8** are basically linkage isomers of the same species, and their formation probably proceeds through different kinetic routes. In intermediate **8**, the pendent phenyl ring comes very close to the metal center, resulting in cyclometalation



by elimination of another HCl. Simultaneously loss of  $\text{PPh}_3$  from the cyclometalated complex occurs, probably triggered by the relatively larger quantity of accumulated HCl, resulting in the formation of a five-coordinate species, which undergoes rapid dimerization through a sulfur bridge to yield the diruthenium complexes. Formation of the two types of complexes from the two different solvents thus appears to be due to domination of either the thione or thiol tautomer in the respective solvents. Difference in the relative concentrations of the two tautomers in the two solvents is evidenced from the difference in the electronic spectral properties (Figure S1) of the thiosemicarbazone ligands in the two solvents. It may be mentioned in this context that the display of different binding modes by thiosemicarbazones in different solvents has precedent in the literature.<sup>[13]</sup>



Scheme 1.



Scheme 2.

All the complexes are diamagnetic, which is consistent with the bivalent state of ruthenium (low-spin  $d^6$ ,  $S = 0$ ) in these complexes. In the  $^1\text{H}$  NMR spectra of the  $[\text{Ru}(\text{PPh}_3)_2(\text{CO})(\text{HLR})(\text{H})]$  complexes the hydride signal is clearly observed as a triplet due to coupling with the two magnetically equivalent phosphorus nuclei near  $-4.5$  ppm. Though the aromatic region of the spectra is a bit complicated due to broad signals displayed by the  $\text{PPh}_3$  ligands ( $7.1$ – $7.7$  ppm), most of the expected signals from the coordinated thiosemicarbazone ligand were identified. The  $^1\text{H}$  NMR spectra of the  $[\text{Ru}_2(\text{PPh}_3)_2(\text{CO})_2(\text{LR})_2]$  complexes show that the two  $\text{Ru}(\text{PPh}_3)(\text{CO})(\text{LR})$  fragments in these dimeric complexes are magnetically equivalent, as has also been indicated in the structural characterization of  $[\text{Ru}_2(\text{PPh}_3)_2(\text{CO})_2(\text{LCl})_2]$ . Besides the absence of the hydride signal, the spectrum of each  $[\text{Ru}_2(\text{PPh}_3)_2(\text{CO})_2(\text{LR})_2]$  complex is qualitatively similar to that of the corresponding  $[\text{Ru}(\text{PPh}_3)_2(\text{CO})(\text{HLR})(\text{H})]$  complex. The  $^1\text{H}$  NMR spectroscopic data of the  $[\text{Ru}(\text{PPh}_3)_2(\text{CO})(\text{HLR})(\text{H})]$  and  $[\text{Ru}_2(\text{PPh}_3)_2(\text{CO})_2(\text{LR})_2]$  complexes are therefore consistent with their composition and stereochemistry.

The infrared spectra of the  $[\text{Ru}(\text{PPh}_3)_2(\text{CO})(\text{HLR})(\text{H})]$  complexes show many vibrations of different intensities in the  $2000$ – $400$   $\text{cm}^{-1}$  region. A strong band near  $1925$   $\text{cm}^{-1}$  indicates the presence of coordinated CO. The Ru–H stretch could not be observed as an isolated signal, as it falls in the same region of the  $\nu(\text{CO})$  stretch, but it appears as a shoulder (near  $1860$   $\text{cm}^{-1}$ ) on the intense  $\nu(\text{CO})$  band. Strong vibrations are also observed near  $746$ ,  $694$ , and  $520$   $\text{cm}^{-1}$ , which are attributed to the  $\text{PPh}_3$  ligands. Comparison with the spectrum of  $[\text{Ru}(\text{PPh}_3)_2(\text{CO})_2\text{Cl}_2]$  shows the presence of some new bands (e.g., bands near  $1589$ ,  $1562$ ,  $1523$ ,  $1302$ , and  $1091$   $\text{cm}^{-1}$ ) in the spectra of the  $[\text{Ru}(\text{PPh}_3)_2(\text{CO})(\text{HLR})(\text{H})]$  complexes, which must be arising due to the coordinated thiosemicarbazone ligand. Infrared spectra of the  $[\text{Ru}_2(\text{PPh}_3)_2(\text{CO})_2(\text{LR})_2]$  complexes are mostly similar to those of the  $[\text{Ru}(\text{PPh}_3)_2(\text{HLR})(\text{CO})(\text{H})]$  complexes.

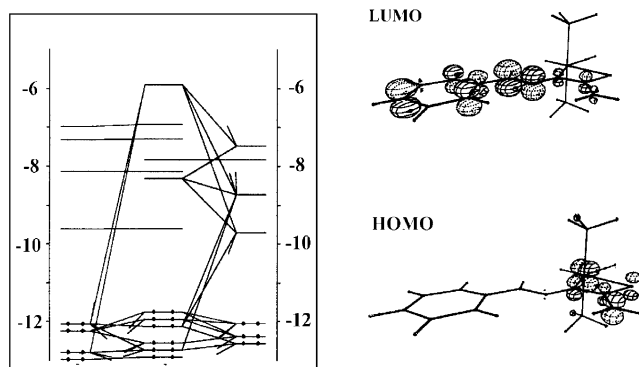
The  $[\text{Ru}(\text{PPh}_3)_2(\text{CO})(\text{HLR})(\text{H})]$  and  $[\text{Ru}_2(\text{PPh}_3)_2(\text{CO})_2(\text{LR})_2]$  complexes are soluble in dichloromethane, chloroform, acetonitrile, acetone, etc., producing intense yellow and orange-yellow solutions, respectively. The electronic spectra of the complexes were recorded in dichloromethane solution. The spectroscopic data are presented in Table 2. Each  $[\text{Ru}(\text{PPh}_3)_2(\text{CO})(\text{HLR})(\text{H})]$  complex shows one intense absorption in the visible region and two intense absorptions<sup>[14]</sup> in the ultraviolet region. The absorptions in the ultraviolet region are assignable to transitions within the ligand orbitals, whereas that in the visible region is probably due to an allowed metal-to-ligand charge-transfer transition. In order to gain insight into the nature of the observed transition in the visible region, qualitative extended Hückel molecular orbital (EHMO) calculations were performed<sup>[15]</sup> on computer-generated models of all the  $[\text{Ru}(\text{PPh}_3)_2(\text{CO})(\text{HLR})(\text{H})]$  complexes, where the phenyl rings of  $\text{PPh}_3$  are replaced by hydrogen atoms. The partial MO diagram for a representative complex is shown in Figure 5 and the composition of selected molecular orbitals is

Table 2. Electronic spectral and cyclic voltammetric data.

Compound	Electronic spectroscopic data <sup>[a]</sup>		Cyclic voltammetric data <sup>[b]</sup>	
	$\lambda_{\text{max}}$ [nm]	( $\epsilon$ , $\text{M}^{-1}\text{cm}^{-1}$ )	$E$ [V] vs. SCE	
[Ru(PPh <sub>3</sub> ) <sub>2</sub> (CO)(HLOCH <sub>3</sub> )(H)]	456 (1850), 342 <sup>[c]</sup>	(9600), 310 (14000)	0.51 <sup>[d]</sup> (80) <sup>[e]</sup>	1.12 <sup>[f]</sup>
[Ru(PPh <sub>3</sub> ) <sub>2</sub> (CO)(HLCH <sub>3</sub> )(H)]	466 (1700), 338 <sup>[c]</sup>	(7160), 302 (13200)	0.54 <sup>[d]</sup> (70) <sup>[e]</sup>	1.14 <sup>[f]</sup>
[Ru(PPh <sub>3</sub> ) <sub>2</sub> (CO)(HLH)(H)]	462 (1400), 346 <sup>[c]</sup>	(5400), 298 (11000)	0.57 <sup>[d]</sup> (60) <sup>[e]</sup>	1.19 <sup>[f]</sup>
[Ru(PPh <sub>3</sub> ) <sub>2</sub> (CO)(HLCI)(H)]	474 (2500), 346 <sup>[c]</sup>	(9900), 310 (18830)	0.66 <sup>[f]</sup>	1.27 <sup>[f]</sup>
[Ru(PPh <sub>3</sub> ) <sub>2</sub> (CO)(HLNO <sub>2</sub> )(H)]	436 (1610), 302	(11260)	0.73 <sup>[f]</sup>	1.43 <sup>[f]</sup>
[Ru <sub>2</sub> (PPh <sub>3</sub> ) <sub>2</sub> (CO) <sub>2</sub> (LOCH <sub>3</sub> ) <sub>2</sub> ]	456 (4600), 350 <sup>[c]</sup>	(1600), 308 (36400), 276 <sup>[c]</sup>	0.48 <sup>[d]</sup> (70) <sup>[e]</sup>	1.09 <sup>[f]</sup>
[Ru <sub>2</sub> (PPh <sub>3</sub> ) <sub>2</sub> (CO) <sub>2</sub> (LCH <sub>3</sub> ) <sub>2</sub> ]	468 (3200), 348 <sup>[c]</sup>	(10900), 310 <sup>[c]</sup> (23000), 274 <sup>[c]</sup>	0.53 <sup>[d]</sup> (80) <sup>[e]</sup>	1.18 <sup>[f]</sup>
[Ru <sub>2</sub> (PPh <sub>3</sub> ) <sub>2</sub> (CO) <sub>2</sub> (LH) <sub>2</sub> ]	472 (2900), 350 <sup>[c]</sup>	(14000), 304 <sup>[c]</sup> (30000), 274 <sup>[c]</sup>	0.56 <sup>[d]</sup> (70) <sup>[e]</sup>	1.20 <sup>[f]</sup>
[Ru <sub>2</sub> (PPh <sub>3</sub> ) <sub>2</sub> (CO) <sub>2</sub> (LCI) <sub>2</sub> ]	468 (2700), 350 <sup>[c]</sup>	(25100), 292 <sup>[c]</sup> (42000), 274 <sup>[c]</sup>	0.55 <sup>[d]</sup> (80) <sup>[e]</sup>	1.23 <sup>[f]</sup>
[Ru <sub>2</sub> (PPh <sub>3</sub> ) <sub>2</sub> (CO) <sub>2</sub> (LNO) <sub>2</sub> ]	562 (2800), 396 <sup>[c]</sup>	(8800), 352 <sup>[c]</sup> (10090), 270 <sup>[c]</sup>	0.72 <sup>[d]</sup> (80) <sup>[e]</sup>	1.47 <sup>[f]</sup>

[a] Dichloromethane solution. [b] Dichloromethane/acetonitrile (1:19), TBAP supporting electrolyte. [c] Shoulder. [d]  $E_{1/2} = 0.5 (E_{\text{pa}} + E_{\text{pc}})$ , where  $E_{\text{pa}}$  and  $E_{\text{pc}}$  are anodic and cathodic peak potentials, respectively. [e]  $\Delta E_p = E_{\text{pa}} - E_{\text{pc}}$  in mV. [f]  $E_{\text{pa}}$  value.

presented in Table S2. Results of these calculations were found to be similar for all the complexes. The highest occupied molecular orbital (HOMO) has a major (64–80%) contribution from the ruthenium  $t_2$  orbitals and the lowest unoccupied molecular orbital (LUMO) is localized almost entirely (95–97%) on the thiosemicarbazone ligand, where a considerable contribution ( $\approx 55\%$ ) comes from the uncoordinated imine fragment.<sup>[16]</sup> Therefore, the absorption in the visible region may be assigned to the charge-transfer transition occurring from the filled ruthenium  $t_2$  orbital (HOMO) to the vacant  $\pi^*$ (imine)-orbital of the thiosemicarbazone ligand (LUMO). The electronic spectral properties of the [Ru<sub>2</sub>(PPh<sub>3</sub>)<sub>2</sub>(CO)<sub>2</sub>(LR)<sub>2</sub>] complexes were found to be similar to those of the [Ru(PPh<sub>3</sub>)<sub>2</sub>(CO)(HLR)(H)] complexes. EHMO calculations of the [Ru<sub>2</sub>(PPh<sub>3</sub>)<sub>2</sub>(CO)<sub>2</sub>(LR)<sub>2</sub>] complexes also support the similarity. The HOMO is again concentrated largely on the metal center and the LUMO is delocalized mostly on the thiosemicarbazone ligands (Figure S2, Table S2). Hence, the absorption in the visible region is assigned to a metal-to-thiosemicarbazone charge-transfer transition, and those in the ultraviolet region are believed to be due to intraligand transitions.

Figure 5. Partial molecular orbital diagram of [Ru(PPh<sub>3</sub>)<sub>2</sub>(CO)(HLH)(H)].

Electrochemical properties of the [Ru(PPh<sub>3</sub>)<sub>2</sub>(CO)(HLR)(H)] and [Ru<sub>2</sub>(PPh<sub>3</sub>)<sub>2</sub>(CO)<sub>2</sub>(LR)<sub>2</sub>] complexes were studied by cyclic voltammetry. The voltammetric data are presented in Table 2 and selected voltammograms are

shown in Figures S3 and S4. Each complex shows two oxidative responses on the positive side of SCE. For the three [Ru(PPh<sub>3</sub>)<sub>2</sub>(CO)(HLR)(H)] complexes, where R = OCH<sub>3</sub>, CH<sub>3</sub>, and H, this oxidation is observed to be reversible, characterized by a peak-to-peak separation ( $\Delta E_p$ ) of 60–80 mV, which remains unchanged upon variation in scan rates, whereas for others this oxidation is irreversible. The first oxidation is reversible in the case of the [Ru<sub>2</sub>(PPh<sub>3</sub>)<sub>2</sub>(CO)<sub>2</sub>(LR)<sub>2</sub>] complexes, with  $\Delta E_p = 70$ –80 mV. For the reversible oxidations, the values of  $\Delta E_p$  remain unchanged upon variation in the scan rate and  $i_{\text{pa}} = i_{\text{pc}}$ . For the remaining two [Ru(PPh<sub>3</sub>)<sub>2</sub>(CO)(HLR)(H)] (R = Cl and NO<sub>2</sub>) complexes, this oxidation is found to be irreversible. In view of the composition of the HOMO, the first oxidative response is assigned to Ru<sup>II</sup>–Ru<sup>III</sup> oxidation. The second oxidative response is irreversible for all the complexes and this is tentatively assigned to Ru<sup>III</sup>–Ru<sup>IV</sup> oxidation. The one-electron nature of both oxidations was established by comparing their current heights ( $i_{\text{pa}}$ ) with those of standard ferrocene–ferrocenium couple under identical experimental conditions. The potential of both the Ru<sup>II</sup>–Ru<sup>III</sup> and Ru<sup>III</sup>–Ru<sup>IV</sup> oxidations is found to be sensitive to the nature of the R substituent in the thiosemicarbazone ligands. The potential increases with increasing electron-withdrawing character of R. The plots of the oxidation potentials ( $E_{\text{pa}}$ ) for both the Ru<sup>II</sup>–Ru<sup>III</sup> and Ru<sup>III</sup>–Ru<sup>IV</sup> couples versus the Hammett substituent constant ( $\sigma$ ) of R<sup>[17]</sup> [ $\sigma$  values of the substituents are OCH<sub>3</sub> = –0.27, CH<sub>3</sub> = –0.17, H = 0.00, Cl = 0.23, NO<sub>2</sub> = 0.78] are linear (Figure S3). The slope of these lines, which is known as the reaction constant ( $\rho$ )<sup>[18]</sup> and is a measure of the sensitivity of the oxidation potentials with R, is 0.17 for the Ru<sup>II</sup>–Ru<sup>III</sup> oxidation and 0.30 for the Ru<sup>III</sup>–Ru<sup>IV</sup> oxidation for the [Ru(PPh<sub>3</sub>)<sub>2</sub>(CO)(HLR)(H)] complex. The values for the [Ru<sub>2</sub>(PPh<sub>3</sub>)<sub>2</sub>(CO)<sub>2</sub>(LR)<sub>2</sub>] complexes are 0.21 and 0.33, respectively. The potential of both the oxidations is found to correlate linearly with the Hammett substituent constant ( $\sigma$ ) of the substituent R in the thiosemicarbazone ligands (Figure S4). This indicates that the Ru<sup>III</sup>–Ru<sup>IV</sup> oxidation potential is more sensitive to the nature of R. It is interesting to note that a single substituent, which is four bonds away from the electroactive metal center, can still influence the metal-centered redox potentials in a predictable manner.

## Conclusions

The present study shows that the coordination mode of benzaldehyde thiosemicarbazones ( $H_2LR$ ) can be manipulated by simply varying the experimental conditions used for the synthesis of their complexes. This has been manifested in the reaction of benzaldehyde thiosemicarbazones with  $[Ru(PPh_3)_2(CO)_2Cl_2]$  under different experimental conditions affording monomeric  $[Ru(PPh_3)_2(CO)(HLR)-(H)]$  and dimeric  $[Ru_2(PPh_3)_2(CO)_2(LR)_2]$  complexes. The monomeric hydride complexes appear suitable for exploring reactivities of the Ru–H bond and such studies are currently in progress.

## Experimental Section

**General Procedure:** Commercial ruthenium trichloride, purchased from Arora Matthey, Kolkata, India, was converted into  $RuCl_3 \cdot 3H_2O$  by repeated evaporation with concentrated hydrochloric acid. Triphenylphosphane was purchased from Loba Chemie, Mumbai, India.  $[Ru(PPh_3)_2(CO)_2Cl_2]$  was synthesized following a reported procedure.<sup>[19]</sup> Benzaldehyde, *para*-substituted benzaldehydes and thiosemicarbazide were obtained from S.D. Fine-Chem, Mumbai, India. The thiosemicarbazone ligands were prepared by treating equimolar amounts of thiosemicarbazide and the respective *para*-substituted benzaldehyde in an ethanol/water (1:1) mixture. All other chemicals and solvents were reagent grade commercial materials and were used as received. Purification of dichloromethane and acetonitrile, and preparation of tetrabutylammonium perchlorate (TBAP) for electrochemical work were performed as reported in the literature.<sup>[20]</sup> Microanalyses (C, H, N) were performed by using a Heraeus Carlo Erba 1108 elemental analyzer. IR spectra were obtained with a Perkin–Elmer 783 spectrometer with samples prepared as KBr pellets. Electronic spectra were recorded with a JASCO V-570 spectrophotometer. Magnetic susceptibilities were measured by using a PAR 155 vibrating sample magnetometer fitted with a Walker scientific L75FBAL magnet.  $^1H$  NMR spectra were recorded in  $CDCl_3$  solution with a Bruker drx 500 NMR spectrometer by using TMS as the internal standard. Electrochemical measurements were done in dichloromethane/acetonitrile (1:9) solution (0.1 M TBAP) by using a CH Instruments model 600A electrochemical analyzer. As the complexes have poor solubility in acetonitrile, a little dichloromethane was initially employed to take them into solution. The presence of acetonitrile in large excess was necessary for recording the redox responses in proper shape, as the responses become distorted in pure dichloromethane solution. A platinum disc working electrode, a platinum wire auxiliary electrode, and an aqueous saturated calomel reference electrode (SCE) were used in a three-electrode configuration. Electrochemical measurements were made under a nitrogen atmosphere. All electrochemical data were collected at 298 K and are uncorrected for junction potentials.

**$[Ru(PPh_3)_2(CO)(HLNO_2)(H)]$ :** To a solution of  $H_2LNO_2$  (32 mg, 0.14 mmol) in ethanol (30 mL) was added  $[Ru(PPh_3)_2(CO)_2Cl_2]$  (100 mg, 0.14 mmol), and the mixture was heated at reflux for 24 h to afford a red solution. The solvent was then evaporated under reduced pressure, and the solid mass thus obtained was purified by thin-layer chromatography on a silica plate by using benzene as the eluant. An orange band separated, which was extracted with acetonitrile. Evaporation of the acetonitrile extract gave  $[Ru(PPh_3)_2(CO)(HLNO_2)(H)]$  as an orange microcrystalline solid. Yield: 93 mg (80%). IR (KBr):  $\tilde{\nu} = 1925$  ( $\nu_{CO}$ ), 1860 ( $\nu_H$ , overlapped with

carbonyl stretch), 746 ( $\nu_{PPh_3}$ ), 694 ( $\nu_{PPh_3}$ ), 520 ( $\nu_{PPh_3}$ ), 1589, 1562, 1523, 1302, 1091  $cm^{-1}$ .  $^1H$  NMR<sup>[21]</sup> (300 MHz,  $CDCl_3$ ):  $\delta = -4.47$  (t,  $J = 19.2$  Hz, 1 H, hydride), 5.19 (s, 2 H,  $NH_2$ ), 7.10 (3 H)\*, 7.25–7.70 (2  $PPh_3$ ), 7.99 (d,  $J = 8.6$  Hz, 2 H) ppm.  $C_{45}H_{38}N_4O_3P_2RuS$  (877.5): calcd. C 61.57, H 4.33, N 6.38; found C 61.54, H 4.34, N 6.37.

**$[Ru(PPh_3)_2(CO)(HLCI)(H)]$ :** This complex was prepared by following the above procedure by using  $H_2LCl$  instead of  $H_2LNO_2$ . Purification of the complex was achieved by thin-layer chromatography on a silica plate by using benzene/acetonitrile (10:1) as the eluant. A yellow band separated, which was extracted with acetonitrile. Evaporation of the acetonitrile extract afforded  $[Ru(PPh_3)_2(CO)(HLCI)(H)]$  as a yellow crystalline solid. Yield: 90 mg (78%). IR (KBr):  $\tilde{\nu} = 1924$  ( $\nu_{CO}$ ), 1861 ( $\nu_H$ , overlapped with carbonyl stretch), 746 ( $\nu_{PPh_3}$ ), 694 ( $\nu_{PPh_3}$ ), 520 ( $\nu_{PPh_3}$ ), 1587, 1561, 1520, 1300, 1094  $cm^{-1}$ .  $^1H$  NMR (300 MHz,  $CDCl_3$ ):  $\delta = -4.61$  (t,  $J = 19.0$  Hz, 1 H, hydride), 5.18 (s, 2 H,  $NH_2$ ), 7.09 (3 H)\*, 7.25–7.70 (2  $PPh_3$ ), 7.97 (d,  $J = 8.6$  Hz, 2 H) ppm.  $C_{45}H_{37}ClN_3OP_2RuS$  (866): calcd. C 62.35, H 4.27, N 4.85; found C 62.37, H 4.37, N 4.88.

**$[Ru(PPh_3)_2(CO)(HLH)(H)]$ :** This complex was prepared by following the procedure for the preparation of  $[Ru(PPh_3)_2(CO)(HLCI)(H)]$  by using the  $H_2LH$  ligand instead of  $H_2LCl$ . Yield: 83 mg (75%). IR (KBr):  $\tilde{\nu} = 1925$  ( $\nu_{CO}$ ), 1860 ( $\nu_H$ , overlapped with carbonyl stretch), 746 ( $\nu_{PPh_3}$ ), 694 ( $\nu_{PPh_3}$ ), 520 ( $\nu_{PPh_3}$ ), 1586, 1563, 1519, 1301, 1095  $cm^{-1}$ .  $^1H$  NMR (300 MHz,  $CDCl_3$ ):  $\delta = -4.57$  (t,  $J = 19.1$  Hz, 1 H, hydride), 5.18 (s, 2 H,  $NH_2$ ), 6.30 (d,  $J = 9.0$  Hz, 1 H), 6.60 (s, 1 H, azomethine proton), 6.73 (2 H)\*, 7.25–7.70 (2  $PPh_3$ ) ppm.  $C_{45}H_{39}N_3OP_2RuS$  (831.5): calcd. C 64.90, H 4.68, N 5.05; found C 64.91, H 4.66, N 5.00.

**$[Ru(PPh_3)_2(CO)(HLCH_3)(H)]$ :** This complex was prepared by following the procedure for the preparation of  $[Ru(PPh_3)_2(CO)(HLCI)(H)]$  by using the  $H_2LCH_3$  ligand instead of  $H_2LCl$ . Yield: 87 mg (77%). IR (KBr):  $\tilde{\nu} = 1925$  ( $\nu_{CO}$ ), 1860 ( $\nu_H$ , overlapped with carbonyl stretch), 746 ( $\nu_{PPh_3}$ ), 694 ( $\nu_{PPh_3}$ ), 520 ( $\nu_{PPh_3}$ ), 1586, 1564, 1519, 1301, 1095  $cm^{-1}$ .  $^1H$  NMR (300 MHz,  $CDCl_3$ ):  $\delta = -4.61$  (t,  $J = 18.9$  Hz, 1 H, hydride), 1.98 (s, 3 H, methyl), 5.19 (s, 2 H,  $NH_2$ ), 6.27 (d,  $J = 8.9$  Hz, 1 H), 6.59 (s, 1 H, azomethine proton), 6.67 (d,  $J = 7.8$  Hz, 1 H), 7.11–7.36 (2  $PPh_3$ ) ppm.  $C_{46}H_{41}N_3OP_2RuS$  (845.5): calcd. C 65.25, H 4.85, N 4.97; found C 65.24, H 4.85, N 4.97.

**$[Ru(PPh_3)_2(CO)(HLOCH_3)(H)]$ :** This complex was prepared by following the procedure for the preparation of  $[Ru(PPh_3)_2(CO)(HLCI)(H)]$  by using the  $H_2LOCH_3$  ligand instead of  $H_2LCl$ . Yield: 94 mg (82%). IR (KBr):  $\tilde{\nu} = 1924$  ( $\nu_{CO}$ ), 1860 ( $\nu_H$ , overlapped with carbonyl stretch), 746 ( $\nu_{PPh_3}$ ), 694 ( $\nu_{PPh_3}$ ), 520 ( $\nu_{PPh_3}$ ), 1586, 1564, 1519, 1301, 1096  $cm^{-1}$ .  $^1H$  NMR (300 MHz,  $CDCl_3$ ):  $\delta = -4.60$  (t,  $J = 8.0$  Hz, 1 H, hydride), 3.10 (s, 3 H, methoxy), 5.19 (s, 2 H,  $NH_2$ ), 6.17 (d,  $J = 8.8$  Hz, 1 H), 6.49 (s, 1 H, azomethine proton), 6.60 (d,  $J = 8.4$  Hz, 1 H), 7.01–7.26 (2  $PPh_3$ ) ppm.  $C_{46}H_{42}N_3O_2P_2RuS$  (861.5): calcd. C 64.03, H 4.76, N 4.88; found C 64.04, H 4.77, N 4.87.

**General Procedure for the Preparation of  $[Ru_2(PPh_3)_2(CO)_2(LR)_2]$ :**  $[Ru(PPh_3)_2(CO)_2Cl_2]$  (100 mg, 0.14 mmol) and  $H_2LR$  (0.14 mmol) were taken up in toluene (30 mL). The mixture was heated at reflux for 25 h to afford a yellow solution (brown in the case of  $R = NO_2$ ). The solvent was then evaporated under reduced pressure, and the solid mass obtained was purified by thin-layer chromatography on a silica plate by using acetonitrile/benzene (1:10) as the eluant. A yellow (purplish-brown in the case of  $R = NO_2$ ) band separated, which was extracted with acetonitrile; evaporation of the acetonitrile extract afforded an orange (purplish-brown in the case of  $R = NO_2$ ) crystalline solid.



Table 3. Crystallographic data for [Ru(PPh<sub>3</sub>)<sub>2</sub>(CO)(HLNO<sub>2</sub>(H))·CH<sub>3</sub>CN and [Ru<sub>2</sub>(PPh<sub>3</sub>)<sub>2</sub>(CO)<sub>2</sub>(LCl)<sub>2</sub>]·2CH<sub>2</sub>Cl<sub>2</sub>.

	[Ru(PPh <sub>3</sub> ) <sub>2</sub> (CO)(HLNO <sub>2</sub> (H))·CH <sub>3</sub> CN	[Ru <sub>2</sub> (PPh <sub>3</sub> ) <sub>2</sub> (CO) <sub>2</sub> (LCl) <sub>2</sub> ]·2CH <sub>2</sub> Cl <sub>2</sub>
Empirical formula	C <sub>47</sub> H <sub>41</sub> N <sub>5</sub> O <sub>3</sub> P <sub>2</sub> SRu	C <sub>56</sub> H <sub>46</sub> Cl <sub>6</sub> N <sub>6</sub> O <sub>2</sub> P <sub>2</sub> S <sub>2</sub> Ru <sub>2</sub>
Formula mass	918.92	1375.89
Crystal system	triclinic	monoclinic
Space group	<i>P</i> $\bar{1}$	<i>P</i> 2 <sub>1</sub> / <i>c</i>
<i>a</i> [Å]	9.4870(15)	12.7896(4)
<i>b</i> [Å]	13.707(3)	24.2852(7)
<i>c</i> [Å]	17.923(4)	18.7290(5)
$\alpha$ [°]	103.83(2)	90
$\beta$ [°]	99.911(15)	99.635(1)
$\gamma$ [°]	98.617(11)	90
<i>V</i> [Å <sup>3</sup> ]	2184.3(7)	5735.1(3)
<i>Z</i>	2	4
$\lambda$ [Å]	0.71073	0.71073
Crystal size [mm]	0.40 × 0.12 × 0.08	0.40 × 0.30 × 0.30
<i>T</i> [K]	293(2)	150(1)
$\mu$ [mm <sup>-1</sup> ]	0.527	0.983
<i>R</i> <sub>1</sub> <sup>[a]</sup>	0.0639	0.0351
<i>wR</i> <sub>2</sub> <sup>[b]</sup>	0.1020	0.0971
GOF <sup>[c]</sup>	0.940	1.079

[a]  $R_1 = \Sigma ||F_o| - |F_c|| / \Sigma |F_o|$ . [b]  $wR_2 = \{\Sigma [w(F_o^2 - F_c^2)^2] / \Sigma [w(F_o^2)^2]\}^{1/2}$ . [c]  $GOF = [\Sigma [w(F_o^2 - F_c^2)^2] / (M - N)]^{1/2}$ , where *M* is the number of reflections and *N* is the number of parameters refined.

**[Ru<sub>2</sub>(PPh<sub>3</sub>)<sub>2</sub>(CO)<sub>2</sub>(LNO<sub>2</sub>)<sub>2</sub>]:** Yield: 125 mg (77%). IR (KBr):  $\tilde{\nu}$  = 1914 ( $\nu_{CO}$ ), 743 ( $\nu_{PPh_3}$ ), 694 ( $\nu_{PPh_3}$ ), 519 ( $\nu_{PPh_3}$ ), 1480, 1432, 1307, 1092 cm<sup>-1</sup>. <sup>1</sup>H NMR (300 MHz, CDCl<sub>3</sub>):  $\delta$  = 4.27 (s, 2 H, NH<sub>2</sub>), 6.83 (d, *J* = 6.0 Hz, 1 H), 7.23–7.46 (PPh<sub>3</sub>), 7.75 (s, 1 H, azomethine proton) ppm. C<sub>54</sub>H<sub>42</sub>N<sub>8</sub>O<sub>6</sub>P<sub>2</sub>Ru<sub>2</sub>S<sub>2</sub> (1227): calcd. C 52.85, H 3.43, N 9.13; found C 52.86, H 3.42, N 9.13.

**[Ru<sub>2</sub>(PPh<sub>3</sub>)<sub>2</sub>(CO)<sub>2</sub>(LCl)<sub>2</sub>]:** Yield: 123 mg (79%). IR (KBr):  $\tilde{\nu}$  = 1914 ( $\nu_{CO}$ ), 743 ( $\nu_{PPh_3}$ ), 694 ( $\nu_{PPh_3}$ ), 519 ( $\nu_{PPh_3}$ ), 1480, 1433, 1307, 1092 cm<sup>-1</sup>. <sup>1</sup>H NMR (300 MHz, CDCl<sub>3</sub>):  $\delta$  = 3.80 (s, 2 H, NH<sub>2</sub>), 6.56 (d, *J* = 6.1 Hz, 1 H), 6.84 (d, *J* = 6.0 Hz, 1 H), 7.16–7.29 (PPh<sub>3</sub>), 7.78 (s, 1 H, azomethine proton) ppm. C<sub>54</sub>H<sub>42</sub>Cl<sub>2</sub>N<sub>6</sub>O<sub>2</sub>P<sub>2</sub>Ru<sub>2</sub>S<sub>2</sub> (1170.5): calcd. C 53.78, H 3.49, N 6.97; found C 53.77, H 3.48, N 6.99.

**[Ru<sub>2</sub>(PPh<sub>3</sub>)<sub>2</sub>(CO)<sub>2</sub>(LH<sub>2</sub>)<sub>2</sub>]:** Yield: 122 mg (80%). IR (KBr):  $\tilde{\nu}$  = 1914 ( $\nu_{CO}$ ), 743 ( $\nu_{PPh_3}$ ), 694 ( $\nu_{PPh_3}$ ), 519 ( $\nu_{PPh_3}$ ), 1479, 1433, 1308, 1092 cm<sup>-1</sup>. <sup>1</sup>H NMR (300 MHz, CDCl<sub>3</sub>):  $\delta$  = 3.80 (s, 2 H, NH<sub>2</sub>), 6.44 (d, *J* = 6.2 Hz, 1 H), 6.85 (d, *J* = 5.9 Hz, 1 H), 7.12–7.28 (PPh<sub>3</sub>), 7.77 (s, 1 H, azomethine proton) ppm. C<sub>54</sub>H<sub>44</sub>N<sub>6</sub>O<sub>2</sub>P<sub>2</sub>Ru<sub>2</sub>S<sub>2</sub> (1136): calcd. C 57.04, H 3.87, N 7.39; found C 57.00, H 3.88, N 7.40.

**[Ru<sub>2</sub>(PPh<sub>3</sub>)<sub>2</sub>(CO)<sub>2</sub>(LCH<sub>3</sub>)<sub>2</sub>]:** Yield: 115 mg (75%). IR (KBr):  $\tilde{\nu}$  = 1914 ( $\nu_{CO}$ ), 743 ( $\nu_{PPh_3}$ ), 694 ( $\nu_{PPh_3}$ ), 519 ( $\nu_{PPh_3}$ ), 1480, 1432, 1308, 1092 cm<sup>-1</sup>. <sup>1</sup>H NMR (300 MHz, CDCl<sub>3</sub>):  $\delta$  = 1.94 (s, 3 H, methyl), 4.04 (s, 2 H, NH<sub>2</sub>), 6.33 (d, *J* = 6.6 Hz, 1 H), 6.64 (s, 1 H), 6.73 (d, *J* = 6.2 Hz, 1 H), 7.20–7.43 (PPh<sub>3</sub>), 7.78 (s, 1 H, azomethine proton) ppm. C<sub>56</sub>H<sub>48</sub>N<sub>6</sub>O<sub>2</sub>P<sub>2</sub>Ru<sub>2</sub>S<sub>2</sub> (1150): calcd. C 57.73, H 4.12, N 7.22; found C 57.74, H 4.11, N 7.24.

**[Ru<sub>2</sub>(PPh<sub>3</sub>)<sub>2</sub>(CO)<sub>2</sub>(LOCH<sub>3</sub>)<sub>2</sub>]:** Yield: 121 mg (78%). IR (KBr):  $\tilde{\nu}$  = 1914 ( $\nu_{CO}$ ), 743 ( $\nu_{PPh_3}$ ), 694 ( $\nu_{PPh_3}$ ), 519 ( $\nu_{PPh_3}$ ), 1481, 1433, 1307.6, 1091 cm<sup>-1</sup>. <sup>1</sup>H NMR (300 MHz, CDCl<sub>3</sub>):  $\delta$  = 3.20 (3 H, methoxy), 4.04 (s, 2 H, NH<sub>2</sub>), 6.27 (d, *J* = 6.5 Hz, 1 H), 6.61 (s, 1 H), 6.70 (d, *J* = 6.0 Hz, 1 H), 7.20–7.43 (PPh<sub>3</sub>), 7.78 (s, 1 H, azomethine proton) ppm. C<sub>56</sub>H<sub>48</sub>N<sub>6</sub>O<sub>4</sub>P<sub>2</sub>Ru<sub>2</sub>S<sub>2</sub> (1166): calcd. C 56.19, H 4.01, N 7.02; found C 56.20, H 4.00, N 7.01.

#### X-ray Crystallography

**[Ru(PPh<sub>3</sub>)<sub>2</sub>(CO)(HLNO<sub>2</sub>(H))·CH<sub>3</sub>CN]:** Single crystals were grown by slow evaporation of an acetonitrile solution of the complex. Se-

lected crystal data and data collection parameters are given in Table 3. Data were collected with a SMART CCD diffractometer by using Mo-*K* $\alpha$  ( $\lambda$  = 0.71073 Å) radiation. The data were corrected for absorption by using SADABS. X-ray data reduction, structure solution, and refinement were done with the use of the SHELXS-97 and SHELXL-97 packages.<sup>[22]</sup> Hydrogen atoms were placed geometrically and positional parameters were refined by using a riding model. The hydride was located from difference syntheses and refined isotropically. The structure was solved by the direct methods.

**[Ru<sub>2</sub>(PPh<sub>3</sub>)<sub>2</sub>(CO)<sub>2</sub>(LCl)<sub>2</sub>]·2CH<sub>2</sub>Cl<sub>2</sub>:** Single crystals were grown by slow diffusion of hexane into a dichloromethane solution of the complex. Selected crystal data and data collection parameters are given in Table 3. Data were collected as above and semiempirical absorption correction was performed by multiscan. X-ray data reduction, structure solution, and refinement were done as above.

CCDC-683479 and -683480 contain the supplementary crystallographic data for this paper. These data can be obtained free of charge from The Cambridge Crystallographic Data Centre via [www.ccdc.cam.ac.uk/data\\_request/cif](http://www.ccdc.cam.ac.uk/data_request/cif).

**Supporting Information** (see footnote on the first page of this article): Hydrogen-bonding parameters; composition of selected molecular orbitals for all complexes; electronic spectra of H<sub>2</sub>LCl in ethanol and toluene; partial molecular orbital diagram of [Ru<sub>2</sub>(PPh<sub>3</sub>)<sub>2</sub>(CO)<sub>2</sub>(LH)<sub>2</sub>]; cyclic voltammograms of [Ru(PPh<sub>3</sub>)<sub>2</sub>(CO)(HLH)(H)] and [Ru<sub>2</sub>(PPh<sub>3</sub>)<sub>2</sub>(CO)<sub>2</sub>(LCH<sub>3</sub>)<sub>2</sub>] and least-squares plots of *E*<sub>pa</sub> values of ruthenium(II)–ruthenium(III) and ruthenium(III)–ruthenium(IV) couples vs.  $\sigma$ .

#### Acknowledgments

Financial assistance received from the Council of Scientific and Industrial Research, New Delhi, India [Grant No. 01(1952)/04/EMR-II] is gratefully acknowledged. The authors thank the referees for their critical comments and constructive suggestions, which have been of great help in preparing the revised manuscript. Sincere thanks are due to Professor S. Lahiri of the Department of Organic Chemistry, Indian Association for the Cultivation of Science, Kolkata, for her help. The authors also thank the Bose Institute, Kolk-



ata 700054, for NMR spectral measurements and the Central Drug Research Institute, Lucknow for elemental analysis. S.D. thanks CSIR for her fellowship [Grant No. 9/96(410)/2003-EMR-I].

- [1] a) M. J. M. Campbell, *Coord. Chem. Rev.* **1975**, *15*, 279; b) S. B. Padhye, G. B. Kaffman, *Coord. Chem. Rev.* **1985**, *63*, 127; c) I. Haiduc, C. Silvestru, *Coord. Chem. Rev.* **1990**, *99*, 253; d) D. X. West, S. B. Padhye, P. B. Sonawane, *Struct. Bonding (Berlin)* **1992**, *76*, 1; e) D. X. West, A. E. Liberta, S. B. Padhye, R. C. Chikate, P. B. Sonawane, A. S. Kumbhar, R. G. Yerande, *Coord. Chem. Rev.* **1993**, *123*, 49.
- [2] a) F. A. French, E. Blanz Jr, *J. Med. Chem.* **1970**, *13*, 1117; b) A. C. Sartorellic, K. C. Agrawal, A. S. Tsiftoglou, A. C. Moore, *Adv. Enz. Reg.* **1977**, *15*, 117; c) K. C. Agrawal, A. C. Sartorelli, *Prog. Med. Chem.* **1978**, *15*, 321; d) J. P. Scovill, D. L. Klayman, C. F. Franchino, *J. Med. Chem.* **1982**, *25*, 1261; e) A. Kraker, S. Krezoski, J. Schneier, D. Mingel, H. Petering, *J. Biol. Chem.* **1985**, *260*, 13710; f) A. E. Liberta, D. X. West, *Biomaterials* **1992**, *5*, 121; g) D. Kovala-Demertzi, A. Domopoulou, M. A. Demertzis, C. P. Raptopoulou, A. Terzis, *Polyhedron* **1994**, *13*, 1917; h) A. Papageorgiou, Z. Iakovidou, D. Mourelatos, E. Mioglou, L. Boutis, A. Kotsis, D. Kovala-Demertzi, D. X. Domopoulou, M. A. Demertzis, *Anticancer Res.* **1997**, *17*, 247; i) M. C. Miller III, C. N. Stineman, J. R. Vance, D. X. West, I. H. Hall, *Anticancer Res.* **1998**, *18*, 4131; j) D. Kovala-Demertzi, J. R. Miller, N. Kourkoumelis, S. K. Hajikakou, M. A. Demertzis, *Polyhedron* **1999**, *18*, 1005; k) Z. Iakovidou, A. Papageorgiou, M. A. Demertzis, E. Mioglou, D. Mourelatos, A. Kotsis, P. N. Yadav, D. Kovala-Demertzi, *Anticancer Drugs* **2001**, *12*, 65.
- [3] a) F. Basuli, S. M. Peng, S. Bhattacharya, *Inorg. Chem.* **1997**, *36*, 5645; b) F. Basuli, M. Ruf, C. G. Pierpont, S. Bhattacharya, *Inorg. Chem.* **1998**, *37*, 613; c) F. Basuli, S. M. Peng, S. Bhattacharya, *Inorg. Chem.* **2000**, *39*, 1120; d) I. Pal, F. Basuli, T. C. W. Mak, S. Bhattacharya, *Angew. Chem. Int. Ed.* **2001**, *40*, 2923; e) S. Dutta, F. Basuli, S. M. Peng, G. H. Lee, S. Bhattacharya, *New J. Chem.* **2002**, *26*, 4623.
- [4] Y. P. Tion, C. Y. Duan, Z. L. Lu, X. Z. You, H. K. Fun, S. Kandasamy, *Polyhedron* **1996**, *15*, 2263.
- [5] a) A. Castineiras, E. Bermejo, D. X. West, A. K. El-Sawaf, J. K. Swearingen, *Polyhedron* **1998**, *17*, 275; b) A. Castineiras, M. Gil, E. Bermejo, D. X. West, *Z. Naturforsch., Teil B* **2000**, *55*, 863; c) E. Bermejo, A. Castineiras, L. J. Ackerman, M. D. Owens, D. X. West, *Z. Allg. Anorg. Chem.* **2001**, *627*, 1966; d) C. A. Brown, W. Kaminsky, K. A. Claborn, K. I. Goldberg, D. X. West, *J. Brazilian Chem. Soc.* **2002**, *13*, 10; e) D. Mishra, S. Naskar, M. G. B. Drew, S. K. Chattopadhyay, *Polyhedron* **2005**, *24*, 1861; f) D. Mishra, S. Naskar, M. G. B. Drew, S. K. Chattopadhyay, *Inorg. Chim. Acta* **2006**, *359*, 585; g) T. S. Lobana, G. Bawa, A. Castineiras, R. J. Butcher, B. J. Liaw, C. W. Liu, *Polyhedron* **2006**, *25*, 2897.
- [6] F. Basuli, S. M. Peng, S. Bhattacharya, *Inorg. Chem.* **2001**, *40*, 1126.
- [7] a) J. J. Levison, S. D. Robinson, *J. Chem. Soc. A* **1970**, 2947; b) R. Young, G. Wilkinson, *Inorg. Synth.* **1977**, *17*, 79; c) R. F. Winter, F. M. Hornung, *Inorg. Chem.* **1997**, *36*, 6197; d) C. S. Yi, S. Y. Yun, I. A. Guzei, *Organometallics* **2004**, *23*, 5392; e) T. Li, R. Churlaud, A. J. Lough, K. Abdur-Rashid, R. H. Morris, *Organometallics* **2004**, *23*, 6239; f) R. CelenligilCetin, L. A. Watson, C. Guo, B. M. Foxman, O. V. Ozerov, *Organometallics* **2005**, *24*, 186.
- [8] a) S. Bhattacharya, C. G. Pierpont, *Inorg. Chem.* **1991**, *30*, 1511; b) M. Menon, A. Pramanik, N. Bag, A. Chakravorty, *J. Chem. Soc., Dalton Trans.* **1995**, 1417; c) A. Pramanik, N. Bag, G. K. Lahiri, A. Chakravorty, *J. Chem. Soc., Dalton Trans.* **1990**, 3823.
- [9] a) A. C. Skapski, P. G. H. Troughton, *Chem. Commun. (London)* **1968**, 1230; b) M. I. Bruce, J. Howard, I. W. Nowell, G. Shaw, P. Woodward, *J. Chem. Soc., Chem. Commun.* **1972**, 1041; c) L. D. Brown, S. D. Robinson, A. Sahajpal, J. A. Ibers, *Inorg. Chem.* **1977**, *16*, 2728.
- [10] a) S. K. Burley, G. A. Petsko, *Science* **1985**, *229*, 23; b) H. C. Weiss, D. Blaser, R. Boese, B. M. Doughan, M. M. Haley, *Chem. Commun.* **1997**, 1703; c) N. N. L. Madhavi, A. K. Katz, H. L. Carrell, A. Nangia, G. R. Desiraju, *Chem. Commun.* **1997**, 1953; d) S. K. Burley, G. A. Petsko, *Adv. Protein Chem.* **1988**, *39*, 125; e) M. Nishio, M. Hirota, Y. Umezawa, *The CH- $\pi$  Interactions (Evidence, Nature and Consequences)*, Wiley-VCH, New York, **1998**; f) Y. Umezawa, S. Tsuboyama, K. Honda, J. Uzawa, M. Nishio, *Bull. Chem. Soc. Jpn.* **1998**, *71*, 1207; g) G. R. Desiraju, T. Steiner, *The Weak hydrogen Bond (IUCr Monograph on Crystallography 9)*, Oxford Science Pub., **1999**; h) M. J. Hannon, C. L. Painting, N. W. Alcock, *Chem. Commun.* **1999**, 2023; i) B. J. Mcnelis, L. C. Nathan, C. J. Clark, *J. Chem. Soc., Dalton Trans.* **1999**, 1831; j) K. Biradha, C. Seward, M. J. Zaworotko, *Angew. Chem. Int. Ed.* **1999**, *38*, 492; k) M. J. Calhorda, *Chem. Commun.* **2000**, 801; l) C. Janiak, S. Temizdemir, S. Dechert, *Inorg. Chem. Commun.* **2000**, *3*, 271; m) C. Janiak, S. Temizdemir, S. Dechert, W. Deck, F. Girgsdies, J. Heinze, M. J. Kolm, T. G. Scarmann, O. M. Zipffel, *Eur. J. Inorg. Chem.* **2000**, 1229; n) T. Steiner, *Angew. Chem. Int. Ed.* **2002**, *41*, 48; o) I. Dance, *New J. Chem.* **2003**, *27*, 22.
- [11] A. Amoedo, M. Graña, J. Martínez, T. Pereira, M. López-Torres, A. Fernández, J. J. Fernández, J. M. Vila, *Eur. J. Inorg. Chem.* **2002**, 613.
- [12] a) H. Yamazaki, K. Aoki, *J. Organomet. Chem.* **1976**, *C54*, 122; b) G. R. Clark, *J. Organomet. Chem.* **1977**, *134*, 51.
- [13] T. S. Lobana, G. Bawa, A. Castineiras, R. J. Butcher, M. Zeller, *Organometallics* **2008**, *27*, 175.
- [14] Only one absorption in the ultraviolet region has been observed in the [Ru(PPh<sub>3</sub>)<sub>2</sub>(CO)(HLNO<sub>2</sub>)(H)] complex.
- [15] a) C. Mealli and D. M. Proserpio, *CACAO Version 4.0*, July, **1994**, Firenze, Italy; b) C. Mealli, D. M. Proserpio, *J. Chem. Educ.* **1990**, *67*, 399.
- [16] J. G. Tojal, T. Rojo, *Polyhedron* **1999**, *18*, 1123.
- [17] L. P. Hammett, *Physical Organic Chemistry*, 2nd ed., McGraw Hill, New York, **1970**.
- [18] R. N. Mukherjee, O. A. Rajan, A. Chakravorty, *Inorg. Chem.* **1982**, *21*, 785.
- [19] A. Ahmed, S. D. Robinson, M. F. Uttley, *J. Chem. Soc., Dalton Trans.* **1972**, 843.
- [20] a) D. T. Sawyer, J. L. Roberts Jr, *Experimental Electrochemistry for Chemists*, Wiley, New York, **1974**, pp. 167–215; b) M. Walter, L. Ramaley, *Anal. Chem.* **1973**, *45*, 165.
- [21] Chemical shifts are given in ppm and multiplicity of the signals along with the associated coupling constants (*J* in Hz) are given in parentheses. Overlapping signals are marked with an asterisk.
- [22] G. M. Sheldrick, *SHELXS-97 and SHELXL-97, Fortran Programs for Crystal Structure Solution and Refinement*, University of Gottingen, **1997**.

Received: May 30, 2008

Published Online: August 29, 2008